DEVELOPMENT OF THE TURBULENT TUBE FLOCCULATOR

A Thesis

Presented to the Faculty of the Graduate School

of Cornell University

in Partial Fulfillment of the Requirements for the Degree of

Master of Science

by

William Pennock

February 2016

ABSTRACT

In this thesis, a dimensionless, composite performance parameter for flocculation in turbulent regimes is proposed. The form of this parameter is $\Gamma\theta\left(\frac{\bar{\varepsilon}}{d_P^2}\right)^{1/3}\phi^{8/9}$, where Γ is the average fractional coverage of primary particles by coagulant, θ is the hydraulic residence time, $\bar{\varepsilon}$ is the average energy dissipation rate, d_P is the average diameter of primary particles, and ϕ is the volume fraction of particles. This composite parameter is complementary to the laminar parameter proposed by Swetland et al. (2014). This parameter is put forth as the basis for a predictive performance model to improve the design of hydraulic flocculators. Model-based design of hydraulic flocculators may lead to improvements in performance as well as more widespread adoption of this energy-efficient technology. In order to test the usefulness of the parameter, a turbulent tube flocculator was designed to have flow conditions analogous to those in the baffled hydraulic flocculators used by Cornell University's AguaClara Program. The design rationale is given, followed by preliminary results obtained with the flocculator. These results lend credence to the usefulness of the turbulent composite parameter, but more data are needed to confirm the applicability of this parameter.

Biographical Sketch

As a junior in high school, William Pennock lacked vocational direction. He had a strong interest in construction and a conviction that his work should be used to help those in need. At the time, it was not clear what would be a suitable occupation that could satisfy both desires. While perusing a course catalog for a local community college, he stumbled upon courses in brick and concrete, which strongly appealed to his inclination toward masonry. He had found the first blaze on his vocational trail.

His investigations soon uncovered civil engineering, a profession he had never known existed, yet which seemed perfectly suited to his interests and abilities. But, could civil engineering help those lacking material resources? He had heard that engineers sit behind desks all day, which didn't sound like a career suited to engaging the needs of others. He found his answer one night while investigating this question when he happened upon the website of Engineering Ministries International, a nonprofit group that donates architecture and engineering services to help build needed infrastructure for communities with limited finances. At that moment, it clicked, he was overwhelmed with joy, and he was decided on a career in engineering. When he learned about environmental engineering and drinking water treatment, his direction was further focused.

William enrolled at the New Jersey Institute of Technology, where he was a civil engineering major with an environmental engineering minor. He quickly became involved with the chapter of Engineers Without Borders there, working on their Biosand Filter project. This experience gave him a first taste of the challenges, complexity, and hope of community water projects. In the summer before his senior year, he interned with HCJB Global in Ecuador, working on clean water projects for indigenous communities. This was William's first work experience in environmental engineering design, and this experience confirmed his intended career trajectory.

At the recommendation of his supervisor at HCJB, William began looking into graduate schools and discovered the AguaClara Program at Cornell University. This became his dream school, and after he visited the AguaClara team at Cornell, he left with a new vision for his academic career. Meeting with Monroe and the team helped him to see that innovation is still needed to optimize water treatment technologies (even "mature" ones) and make them available for all. Gratefully accepted and funded, William came to Cornell in the summer of 2013 to learn how to clean water. Ever since, he has been contentedly flooding the basement of Hollister Hall in the hope of making clean water more globally accessible.

This thesis is dedicated to everyone who actually reads this thesis. When you've read it, send me an e-mail at whp28@cornell.edu; you'll have validated months of my life.

Acknowledgements

To begin, I would like to thank my two advisors, Len and Monroe. I count myself blessed to be under your guidance. You have both taught me a great deal, explicitly and implicitly, academically and personally. I am very grateful for the role you have both played in shaping me as an academic and as an adult. Likewise, I would like to thank Dr. John Schuring of the New Jersey Institute of Technology, who introduced me to research and exemplified incredible mentorship in developing me as a fledgling researcher. I would also like to thank Casey Garland for being an excellent group member and example of what a graduate student should be. In that vein, I would like to thank Karen Swetland, whom I have never met, but whose academic footsteps I am following.

I would next like to thank the students who worked on this project before me and with me: Jonathan Christensen, Felice Chan, Mingze Niu, Stephen Jacobs, Ana Maria Gurgel Oliveira, Amanda Rodriguez, Brooke Pian, and Greta Schneider-Herr. I would like to particularly thank Felice Chan, who worked on this project from the beginning, instituted sarcasm as the lingua franca of the project team, named the apparatus Franklin, sustained team morale with kitten pictures, and did a great deal for this work. I would also like to specially thank Jonathan Christensen for the incredible amount of work he did on the design and construction of the apparatus.

I am grateful to my fellow inhabitants in the basement of Hollister Hall; you make this a fun place to work. I would like to thank Paul Charles and Tim Brock for their practical suggestions, craftsmanship, and conversation. I would also like to thank Cameron Willkens for his patient technical support. The custodial staff have my gratitude for keeping things orderly and for being some of the friendliest and most interesting people I have met at Cornell. I am so glad the newest residents of the basement, the entire AguaClara team, are here. Your energy, dedication, and creativity continuously inspire me.

I would probably not be here if not for the faithful encouragement and investment I receive from home. Thank you, Mom, Dad, Elise, and Andrew for your support and inspiration. Each one of you inspires me in a different way, and I am proud to be part of this family. I would also like to thank Anna and Alexey, my two best friends from undergraduate. Your perseverance in being my friends in my busiest and roughest times has meant more than you know. Rob, you know who you are. I would also like to thank Jonathan Daudelin, my friend and roommate from NJIT and my friend and housemate from Cornell. Thank you for being an incredible housemate and an inspiration to me. It has been an honor and a privilege to live with you these last four years.

Lastly, I would like to thank the groups who welcomed me to Ithaca and helped me find a home in a town of transients. To the members of Graduate Christian Fellowship and Cornell International Christian Fellowship: thank you for welcoming me, challenging me, and uplifting me. Thank you also to the Ithaca Church of Christ, especially Bill, Sharon, and Gregg, for making me feel like family. I conclude with gratitude to my Lord Jesus Christ for His unparalleled love and patience. Soli Deo gloria.

Table of Contents

List of Tables

List of Figures

Chapter 1

Introduction

For the last ten years, the AguaClara Program at Cornell University has been bringing innovation to drinking water treatment technology. This has led to the construction of twelve water treatment plants in Honduras and two in India, serving over 40,000 people. Each successive plant design has been an improvement over the last, but no plant has yet been designed that is completely optimized. In AguaClara's surface water treatment plants, small particles continue to evade the battery of particle-removal processes and impact the quality of drinking water. Flocculation is the process that changes the particle size distribution of the raw water to be more suitable for sedimentation and filtration. Improved flocculation performance, then, could contribute to higher sedimentation and filtration performance, resulting in purer water.

A considerable limitation to achieving high-performing flocculators is limited design guidance, which is reflective of an incomplete understanding of the physical/chemical process of flocculation. In order to create the next generation

of flocculators, strides must be made in understanding what controls and what limits performance of the flocculation process. This has been a central goal of AguaClara research for the last five years.

The contribution of this thesis to the AguaClara Program's work in flocculation is to lay the groundwork for study of flocculation in turbulent conditions. All municipal-scale flocculators operate in the turbulent regime, and so this hydodynamic reality must be accounted for in understanding the flocculation process as it relates to community-scale drinking water treatment. This paper begins by outlining the result of several years of thought on the form of a model for flocculation performance, and expands it to turbulent flocculation, continuing from Karen Swetland's work on laminar flocculation (2014). This culminates in the proposal of a dimensionless composite parameter that could form the foundation of a predictive model for hydraulic flocculator performance. This predictive performance model could then be used to improve designs for hydraulic flocculators as well as guide their operation.

Having laid the foundation for a predictive model of flocculation performance in turbulent conditions, this thesis shows the initial steps in the next phase of this research: testing the descriptive capability of the parameter. This begins with the design of the turbulent tube flocculator, a lab-scale tube flocculator in which the flow is turbulent. After describing the rationale for the design, experimental protocol and initial results are presented. These results are not conclusive, but give an indication of what trends might be observed in further experiments.

This thesis sets the course for a study that should lead to the creation of a predictive performance model for real flocculators. Additional testing of the

composite parameter will be needed to validate its utility in explaining flocculation performance. Further studies will incorporate additional parameters as needed to account for additional phenomena that affect performance of real flocculators, such as the presence of dissolved organic matter. The long term objective for the model is to be able to take flocculator properties and influent water characteristics to predict the turbidity of water leaving the sedimentation tank. Once the model has demonstrated the capacity to predict performance under reasonably realistic flocculation conditions, it will be tested with data from real flocculators in Honduras.

Chapter 2

Development of the Turbulent Tube Flocculator *

2.1 Abstract

A predictive, mechanistically-based performance model for hydraulic flocculation could potentially enable improved design for hydraulic flocculators. Such a model would take the characteristics of the flocculator and the suspension as inputs so that designers and operators could rationally consider the effects of changing flocculator dimensions or influent water conditions on performance. Previous research by Swetland et al. (2014) developed a performance model for laminar flocculators, but a model for turbulent flocculators is still needed, as municipal scale flocculators operate in the turbulent regime. This paper outlines

*The contents of this chapter have been submitted for publication in Environmental Engineering Science with coauthors Felice Chan, Monroe Weber-Shirk, and Leonard Lion.

a theoretical approach that suggests the form of of a dimensionless composite parameter that accounts for the influence of raw water turbidity, coagulant dose, flocculator hydraulic residence time, and energy dissipation rate on settled water turbidity. The utility of this parameter will require testing and validation. Thus, this paper also describes the design of a suitable laboratory test apparatus which produces turbulent flow conditions that mimic those in a baffled hydraulic flocculator. Preliminary experimental results are given which indicate, pending additional testing at varying conditions, that the proposed turbulent composite design parameter may have predictive utility.

2.2 Introduction

Many municipal drinking water treatment plants could benefit from the reduction in operation and maintenance costs that results from using baffled hydraulic flocculators. Unlike mechanical flocculators, baffled hydraulic flocculators require no electricity to operate and have no moving parts that would need to be serviced or replaced in the normal operation of the plant. Energy efficient hydraulic flocculators are not widely implemented, because they are assumed to be less flexible in operation and design guidelines give preference to mechanical flocculators (Haarhoff, 1998; GLUMRB, 2012). Mechanistically-based design guidelines for hydraulic flocculators could lead to more efficient design, more widespread adoption, and decreased costs for municipal drinking water treatment plants.

Weber-Shirk and Lion (2010) developed a fundamentally-based, dimensionless composite parameter to describe the collision potential for a baffled hy-

draulic flocculator. Collision potential is an estimate of the number of collisions the average particle is likely to experience in a given set of conditions. This composite parameter can be used to develop a model for flocculator performance that could lead to lower cost and more efficient designs. The composite parameter was further refined in collaboration with Swetland under conditions of laminar flow, and is defined as shown in Equation 2.1:

$$N_c \propto G\theta\Gamma\phi_0^{2/3}, \tag{2.1}$$

where N_c is the potential number of collisions, G is the velocity gradient (units of Time^{-1}), θ is the hydraulic residence time, and ϕ_0 is the initial volume fraction of particles, the ratio of the initial volume of particles to the volume of the reactor, defined as $\phi_0 = \frac{C_{P_0}}{\rho_P}$ (Swetland et al., 2014), where C_{P_0} is the initial concentration of primary particles in suspension and ρ_P is the density of the primary particles. Last, Γ is the fraction (between 0 and 1) of primary particle surface area that is covered with coagulant precipitates, and it has the same effect as a collision efficiency factor, although with a physical interpretation. The predictive utility of this parameter on settled water turbidity was verified for conditions of laminar flow (Swetland et al., 2014).

In order to make Equation 2.1 more intuitive, the average separation distance between particles can be substituted for particle volume fraction. First, it is noted that ϕ is a ratio of concentration to density, both of which are in units of $\frac{\text{Mass}}{\text{Volume}}$. For both concentration and density, the mass is that of the particles. Therefore, the mass cancels, and ϕ is simplified to a ratio of volumes: the combined volume of the particles to the total volume of reactor. Since the desired relationship is agent-based and focuses on a single hypothetical particle, the ra-

tio described previously can be made to be the ratio of the volume of a single particle to the volume of fluid that surrounds that single particle:

$$\phi = \frac{\forbidden{V}_{\mathrm{P}}}{\forbidden{V}_{\mathrm{Surround}}} = \frac{\frac{\pi}{6} d_{\mathrm{P}}^3}{\Lambda^3}, \tag{2.2}$$

where d_{P} is the diameter of a particle (assuming it is spherical), and Λ is the average separation distance between particles.

The choice of velocity gradient, G, as part of the dimensionless composite parameter is based upon the Camp-Stein formulation (Cleasby, 1984). Nevertheless, this is a result that can be anticipated when describing the relative velocities between particles in a laminar flow. Assuming that the primary particles in flocculation have low inertia such that they accelerate with the surrounding fluid (i.e., low Stokes number), the relative velocity can be assumed to be dependent upon the average energy dissipation rate ($\overline{\varepsilon}$), the kinematic viscosity of the fluid (ν), and the distance separating the particles (Λ):

$$v_{\mathrm{r}} = f(\overline{\varepsilon}, \nu, \Lambda). \tag{2.3}$$

At the scale of typical particle separation distance in laminar flow, shear can be approximated as uniform, and thus the relative velocity varies linearly with separation distance between the particles. Therefore, the equation becomes $v_{\mathrm{r}} \sim \Lambda f(\overline{\varepsilon}, \nu)$. In order for the relative velocity to have the proper units, $f(\overline{\varepsilon}, \nu)$ must have units of $\frac{1}{\mathrm{Time}}$. Because energy dissipation rate has units of $\frac{\mathrm{Length}^2}{\mathrm{Time}^3}$, and kinematic viscosity has units of $\frac{\mathrm{Length}^2}{\mathrm{Time}}$, the necessary formulation of $f(\overline{\varepsilon}, \nu)$ is $\sqrt{\frac{\overline{\varepsilon}}{\nu}}$. This is the definition of G,

$$G = \sqrt{\frac{\overline{\varepsilon}}{\nu}}, \tag{2.4}$$

and so

$$v_{\mathrm{r}} \sim \Lambda G \tag{2.5}$$

in a laminar flow (Cleasby, 1984).

The remaining terms, ϕ and Γ, were included in N_c according to the following reasoning. First, the fluid volume that surrounds a floc is related to the separation distance as:

$$\forall_{\mathrm{Surround}} = \frac{\forall_{\mathrm{P}}}{\phi} = \frac{\pi d_{\mathrm{P}}^3}{6}\frac{\rho_{\mathrm{P}}}{C_{\mathrm{P}}} = \Lambda^3, \tag{2.6}$$

where ρ_{P}, d_{P}, and C_{P} are the density, diameter, and concentration of the primary particles. Making the simplifying assumption that particles occupy cubic volumes, Equation 2.6 gives the average volume of fluid occupied by each particle.

Just as there is an occupied volume associated with each particle, there is a fluid volume associated with each collision (i.e., the volume of water cleared by particle motion before the collision occurred), which is a volume defined by the distance the floc has traveled multiplied by the area of a circle with diameter equal to the sum of the diameters of the particles that collided. Successful collisions are assumed to occur between similarly sized particles, and thus the collision area is $\frac{\pi(2d_{\mathrm{P}})^2}{4} = \pi d_{\mathrm{P}}^2$ and the volume cleared is as follows:

$$\forall_{\text{Cleared}} = \pi d_{\text{P}}^2 v_{\text{r}} t_{\text{c}}, \tag{2.7}$$

where t_{c} is the time it takes for one collision to occur, so that the product $v_{\text{r}} t_{\text{c}}$ is equivalent to the mean free path, the average distance between particle collisions (Crowe, 2005). The average collision time can be considered the time it takes for the volume cleared to equal the suspension volume occupied by a particle. While the actual ratio of $\forall_{\text{Cleared}}$ to $\forall_{\text{Surround}}$ might be less than or greater than 1 for any given collision, this condition is meant to represent an average. Substituting and rearranging this equality, the collision time is defined as:

$$t_{\text{c}} = \frac{\Lambda^3}{\pi d_{\text{P}}^2 v_{\text{r}}}. \tag{2.8}$$

Substituting Equation 2.5 into Equation 2.8 gives the average collision time for particle interactions dominated by viscosity:

$$t_{\text{c}} = \frac{\Lambda^2}{\pi d_{\text{P}}^2 G}. \tag{2.9}$$

The rate of successful collisions that result in aggregation is assumed to be directly proportional to the coagulant precipitate coverage of the primary particles and inversely proportional to the average collision time and is thus defined by:

$$\frac{\mathrm{d}N_c}{\mathrm{d}t} = \frac{\Gamma}{t_{\text{c}}}. \tag{2.10}$$

Substituting the collision time found for laminar flows, Equation 2.9, into Equa-

tion 2.10 gives the differential number of collisions for a laminar flow as:

$$\mathrm{d}N_c = \pi \frac{d_\mathrm{P}^2}{\Lambda^2} \Gamma G \mathrm{d}t. \tag{2.11}$$

This equation can be converted to a form similar to that shown in Equation 2.1 by recognizing that the volume fraction of particles is a ratio of volumes (see Equation 2.2). Taking the cube root of this ratio of volumes and then squaring it shows that the ratio of squared lengths ($\frac{d_\mathrm{P}^2}{\Lambda^2}$) given in Equation 2.11 is proportional to $\phi^{2/3}$.

The same approach can be applied to formulate a composite parameter for the differential number of collisions in turbulent flows. In turbulence, kinematic viscosity is not anticipated to be an important parameter, since inertial forces will dominate viscous forces at length scales larger than the Kolmogorov length scale, η. The Kolmogorov length scale is defined as

$$\eta = \sqrt[4]{\frac{\nu^3}{\varepsilon}}, \tag{2.12}$$

and is representative of the small scales at which viscosity becomes as significant a force as inertial force (Tennekes and Lumley, 1972). Therefore, the use of velocity gradient, G, in Equation 2.1 makes it applicable only to laminar flows or turbulent flows with particle separation distances that are less than the Kolmogorov length scale. All municipal scale flocculators are turbulent, and Cleasby (1984) determined that use of G is not valid in the analysis of turbulent flows where the relevant length scale is larger than the Kolmogorov length scale, η. When particle separation distance is larger than the Kolmogorov length scale, the relationship for relative velocity becomes $v_\mathrm{r} = f(\overline{\varepsilon}, \Lambda)$, since viscous ef-

fects become negligible. Because the units of this relationship must be those of velocity, the formulation becomes

$$v_{\mathrm{r}} \sim \sqrt[3]{\overline{\varepsilon}\Lambda}. \tag{2.13}$$

Thus, while collision rates in laminar flocculation or with particle separation distances smaller than the Kolmogorov length scale are proportional to $\sqrt[2]{\overline{\varepsilon}}$, collision rates at scales larger than the Kolmogorov length scale are proportional to $\sqrt[3]{\overline{\varepsilon}}$. This proportionality has been previously shown to apply to turbulent flows (Tennekes and Lumley, 1972).

Substituting Equation 2.13 into Equation 2.8 yields

$$t_{\mathrm{c}} = \frac{\Lambda^3}{\pi d_{\mathrm{P}}^2 (\Lambda\overline{\varepsilon})^{1/3}}. \tag{2.14}$$

Equation 2.14 can then be substituted into Equation 2.10 to give the differential number of collisions for a turbulent flow as follows:

$$\mathrm{d}N_c = \pi \frac{d_{\mathrm{P}}^2}{\Lambda^2} \left(\frac{\overline{\varepsilon}}{\Lambda^2}\right)^{1/3} \Gamma \mathrm{d}t. \tag{2.15}$$

As with the laminar relationship in Equation 2.11, the successful collision rate in Equation 2.15 can be shown to be proportional to ϕ to some power. This requires a substitution made possible by manipulating Equation 2.6 to become

$$\frac{\Lambda}{d_{\mathrm{P}}} = \left(\frac{\pi}{6}\frac{\rho_{\mathrm{P}}}{C_{\mathrm{P}}}\right)^{1/3} = \left(\frac{\pi}{6}\frac{1}{\phi}\right)^{1/3}. \tag{2.16}$$

Inverting Equation 2.16, squaring it, and substituting it for the $\frac{d_P^2}{\Lambda^2}$ quantity as well as solving Equation 2.16 for Λ, squaring it, and substituting it for the Λ^2 in the denominator of the $\left(\frac{\bar{\varepsilon}}{\Lambda^2}\right)^{1/3}$ quantity changes Equation 2.15 to:

$$dN_c = (6^{11/9}\pi^{5/18})\phi^{8/9}\left(\frac{\bar{\varepsilon}}{d_P^2}\right)^{1/3}\Gamma dt. \tag{2.17}$$

Thus, by analogy with Equation 2.11, turbulent flocculation performance is proposed to be a function of:

$$N_c \propto \Gamma\theta\left(\frac{\bar{\varepsilon}}{d_P^2}\right)^{1/3}\phi_0^{8/9}. \tag{2.18}$$

The composite parameter in Equation 2.18 is expected to characterize turbulent flocculation data like Equation 2.1 did for laminar data. This relationship is a continuation of one proposed by Weber-Shirk and Lion (2010), who noted that the composite parameter for turbulent flocculation should be proportional to $\theta\bar{\varepsilon}^{\frac{1}{3}}$. Having proposed a dimensionless composite parameter for turbulent flocculation in Equation 2.18, experiments are needed to test the composite parameter's descriptive power. This necessitated the creation of a lab scale hydraulic flocculator in which flow is turbulent. A discussion of design and construction of the lab scale flocculator is given in the following section.

2.3 Design of Apparatus

In designing the experimental flocculator, the underlying criterion was that the flocculator needed to be representative of the flocculation conditions present

in a full scale baffled hydraulic flocculator. The foremost consideration was that the lab scale version must experience turbulent flow and have the majority of the turbulence generated from flow expansions. Likewise, the laboratory apparatus needed to achieve a high Péclet Number to approximate a plug flow reactor, as baffled hydraulic flocculators do in practice. The design chosen to meet these criteria was a coiled tube flocculator, which is illustrated in Figure 2.1.

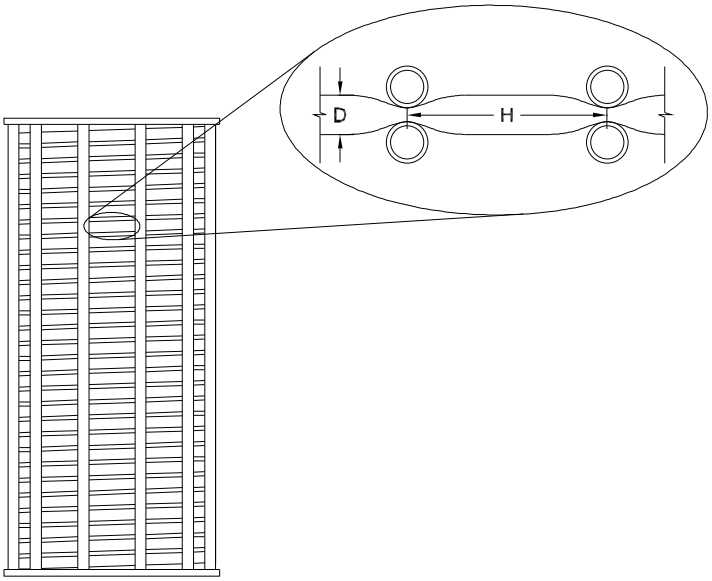

Figure 2.1: Diagram of Apparatus with Inset

Figure 2.1 depicts a coiled tube supported by columns. The inset shows that the twelve vertical supports are also used to constrict the tubing. These constrictions achieve turbulent mixing characteristics analogous to those found in baffled hydraulic flocculators. In the regions following baffles, hydraulic flocculators have zones where the flow contracts and later expands (see Figure 2.2). Thus, the tube constrictions serve the place of baffles in causing the flow to contract and expand.

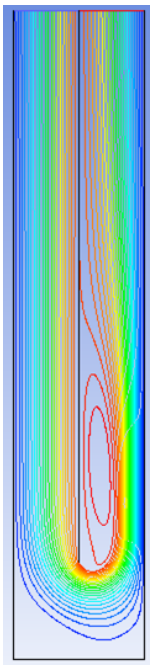

Figure 2.2: Streamlines of Flow Rounding a 180° Bend

The minimum dimensions of the flocculator were determined from the minimum Reynolds number of 4,000 for turbulence in pipe flow and the design mean energy dissipation rate of 15 mW/kg (Granger, 1995). The use of $\mathrm{Re} = 4,000$ is conservative, since constrictions and bends in the tubing will induce turbulence at lower Reynolds numbers. The average energy dissipation rate of 15 mW/kg is equivalent to a velocity gradient, G, of 122.5 s^{-1}, assuming the viscosity of water is 1 mm^2/s. Recommended values of G for baffled hydraulic flocculators fall in the range of 20 to 100 s^{-1}, so the experimental flocculator can achieve more intense mixing than traditional hydraulic flocculators (Schulz and Okun, 1984). One of the aims of this research is to facilitate the development of smaller, more efficient flocculators, and so the ability to explore higher energy dissipation rates was desirable. Lower energy dissipation rates can be achieved by widening of the tube constrictions, and for the initial experiments reported in this study, an average energy dissipation rate of 7.4 mW/kg

(G = 85.8 s^{-1}) was used.

The minimum tube diameter was determined by relating the diameter to the Reynolds number and energy dissipation rate. The derivation of this relationship begins with an expression for average energy dissipation rate, as shown in Equation 2.19:

$$\bar{\varepsilon} = \frac{gh_l}{\theta}, \tag{2.19}$$

where g is gravitational acceleration and h_l is the head loss in the system. The derivation proceeds by substituting terms in Equation 2.19 with equations for head loss and hydraulic residence time. The minor loss equation for head loss,

$$h_l = K\frac{V^2}{2g} \tag{2.20}$$

was used, because the majority of head loss in baffled hydraulic flocculators is caused by losses associated with fluid expansion after contractions of the mean flow (as opposed to major losses - those due to wall shear), and the lab scale flocculator will also be dominated by minor losses (Granger, 1995). The value of K in the minor loss equation will be the minor loss coefficient for a single flow constriction. Haarhoff (1998) found the value of K for a 180° bend to be 2.0, so 2.0 was used for preliminary estimates of minor losses and average energy dissipation rate in the apparatus. The actual value of K in the turbulent tube flocculator is variable, depending upon the degree to which the tubing is constricted.

The hydraulic residence time, θ, for Equation 2.19 was considered to be the

time it takes the flow to travel from one constriction to the next, assuming constriction of the flow volume is negligible, $\theta = \frac{H}{V}$; where H is the distance between constrictions and V is the mean fluid velocity.

Substituting the two aforementioned relationships for minor loss and hydraulic residence time into Equation 2.19 and simplifying yields Equation 2.21.

$$\overline{\varepsilon} = \frac{KV^3}{2H} \tag{2.21}$$

An important parameter in the design of a tubular hydraulic flocculator is the ratio between H, and the diameter of the tubing, D, $\Pi_{HD} = \frac{H}{D}$. In a computational fluid dynamics analysis of baffled hydraulic flocculators (180° bends), Haarhoff and van der Walt (2001) found the optimal value of Π_{HD} (in their case, the ratio of channel length to channel width) to be less than or equal to six for efficient mixing.

The extension of this ratio to the tube flocculator for the case where the constriction of flow is similar to that caused by a 180° bend was supported by geometric calculations based on the spreading rate of plane jets, since the flow after a constriction in a tube flocculator is considered to be a plane jet. The smallest (most conservative) spreading rate found in a literature review by Kotsovinos (1976) was 0.087. Using this spreading rate, the jet was found to expand to the diameter of the tube after traveling a distance less than five diameters in length, as illustrated in Figure 2.3. For this apparatus, $\Pi_{HD} = 4.9$ was used to design the flocculator.

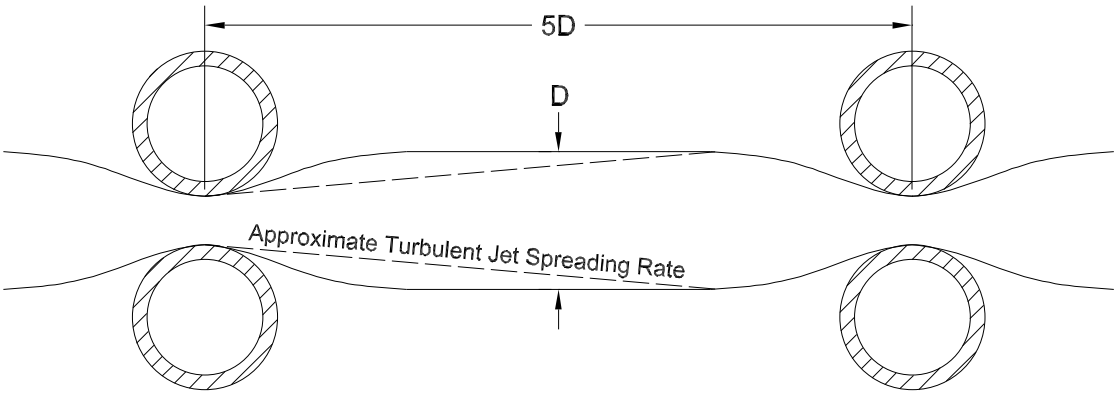

Figure 2.3: Diagram of Estimated Jet Expansion Geometry

Substituting Π_{HD} into Equation 2.21 and solving for velocity leads to Equation 2.22.

$$V = \sqrt[3]{\frac{2\Pi_{HD} D \overline{\varepsilon}}{K}} \tag{2.22}$$

Multiplying both sides of Equation 2.22 by $\frac{D}{\nu}$ results in an equation for Reynolds number (Re). The diameter of the tubing can then be expressed as a function of Re, $\overline{\varepsilon}$, and Π_{HD} by solving Equation 2.22 for D as shown in Equation 2.23.

$$D = \sqrt[4]{\frac{(\nu \mathrm{Re})^3 K}{2\Pi_{HD} \overline{\varepsilon}}} \tag{2.23}$$

Solving Equation 2.23 with a kinematic viscosity (ν) of 1 $\frac{\mathrm{mm}}{\mathrm{s}^2}$, a Reynolds number (Re) of 4,000, a minor loss coefficient (K) of 2.0, a Π_{HD} ratio of 4.9, and an average energy dissipation rate ($\overline{\varepsilon}$) of 15 $\frac{\mathrm{mW}}{\mathrm{kg}}$ results in a minimum diameter of 3.1 cm (1.2 in). For the apparatus, tubing with an inner diameter of 3.18 cm (1.25

in) and an outer diameter of 3.81 cm (1.5 in) was chosen.

The design area of constrictions was calculated based on the constriction of flow around a bend in a hydraulic flocculator. When water flows around a 90° bend, its effective area is reduced to 61% of the total flow area, as represented by the contraction coefficient of 0.61 for sluice gates (Kim, 2007). A 180° bend, such as around a flocculator baffle, is essentially two 90° bends (Haarhoff and van der Walt, 2001). Therefore, the effective area of the flow is reduced to $0.61 \times 0.61 = 0.37$, or 37%, of the total flow area.

The design constriction width was determined from geometric principles, considering the constricted tubing to approximate a rectangle with two semicircles at its ends as shown in Figure 2.4. The problem was formulated as a solution of two simultaneous equations, representing the constraints that the constricted area must be 37% of the unconstricted area and that the circumference of the tubing must remain the same for the center of the tubing wall (i.e., the average diameter, $\frac{D_O+D_I}{2}$, where D_O and D_I are the outer and inner diameters of the unconstricted tube, respectively). The latter assumption considers the center of the tubing wall to coincide with the neutral plane of the tubing. See Figure 2.4 for a diagram of the geometry of the problem.

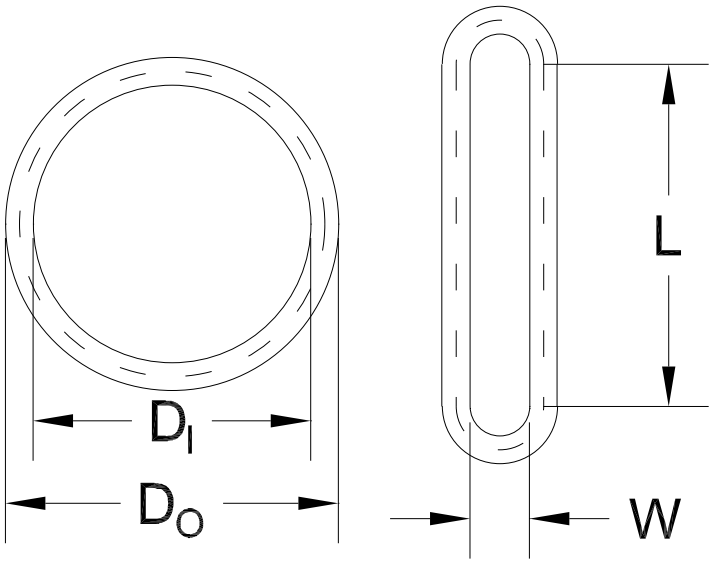

Figure 2.4: Geometry of Tube Constriction

The equation for the length of the centerline of the tubing wall (dashed line in Figure 2.4) being constant is expressed in Equation 2.24:

$$\pi\left(\frac{D_O + D_I}{2}\right) = 2L + \pi\left(W + \frac{D_O - D_I}{2}\right), \tag{2.24}$$

where W is the width of the constricted tube and L is the length of the assumed rectangular portion of the constricted tube. The contraction in the tubing is gradual, and thus it was assumed that there was no additional flow contraction (vena contracta) downstream of the constriction in the tubing. The equation for the area of this flow contraction is given in Equation 2.25:

$$WL + \frac{\pi}{4}W^2 = \Pi_{AR}\frac{\pi}{4}D_I^2, \tag{2.25}$$

where Π_{AR} is the area ratio, the ratio of the constricted area to the unconstricted area, which is equal to 0.37 in this case. Simultaneous solution of Equations 2.24

and 2.25 leads to a quadratic equation that can be solved for W, the width of the constriction as seen in Equation 2.26:

$$W^2 - 2D_I W + \Pi_{AR} D_I^2 = 0. \tag{2.26}$$

In the final solution, the outer diameter D_O is canceled out and only the inner diameter D_I matters (i.e., wall thickness does not affect this solution). Solving Equation 2.26 with D_I as 3.18 cm (1.25 in) gives a constriction width of 0.66 cm (0.26 in). Wall thickness becomes important when selecting the spacing of the vertical bars to constrict the tubing. Adding the difference $D_O - D_I$ to W gives the distance between the vertical bars of 1.30 cm (0.51 in). For the preliminary experiments, the spacing between the bars was 1.56 cm (0.61 in), giving a constriction width of 0.93 cm (0.36 in). Because this is a wider spacing than specified, the assumption that the constricted flow will expand to its full area before the next constriction (see Figure 2.3) is still valid. This spacing achieved an average energy dissipation rate of 7.4 mW/kg in the flocculator. The spacing between constrictions was 15.5 cm (6.1 in) based on 4.9 times the inner diameter of the tubing.

The design flow rate for the flocculator can be found in a manner similar to the way the minimum diameter was found. Setting the left side of Equation 2.22 equal to $\frac{Q}{\frac{\pi}{4}D^2}$ and solving for Q results in Equation 2.27:

$$Q = \frac{\pi}{4}\left(\frac{2\Pi_{HD} D^7 \overline{\varepsilon}}{K}\right)^{1/3}. \tag{2.27}$$

Equation 2.27 can be used to calculate the apparatus flow rate. With the chosen diameter of 3.18 cm (1.25 in) and using the same values used to calculate the

diameter, the design flow rate was 105.0 mL/s. For initial experiments, a flow rate of 109.0 mL/s was selected.

As a last step in design of the flocculator, the tubing length was chosen. This was set at 56.35 m in order to achieve a similar product of residence time and average energy dissipation rate to the one-third power ($\theta\overline{\varepsilon}^{1/3}$) to that which is used in the Cornell University AguaClara Program design for baffled hydraulic flocculators that have been constructed in Honduras. A summary of the values chosen for the final design of the flocculator can be found in Table 2.1. A pulse input test conducted on the flocculator found a Péclet number of about 91, indicating that advection dominates dispersion in this reactor, and this flocculator is plug flow, as intended.

Table 2.1: Tube Flocculator Design Parameters

Design Parameter	**Symbol**	**Chosen Value**
Inner Diameter (cm)	D_{I}	3.18
Flow Rate (mL/s)	Q	109
Reynolds Number	Re	4,371
Mean Energy Dissipation Rate (mW/kg)	$\overline{\varepsilon}$	7.4
Length (m)	L	56.35
Residence time (s)	θ	409.3

Flow through an orifice prior to the flocculator was used to achieve rapid mix of coagulant with the raw water, which was created by adding kaolinite clay to Cornell University tap water. The energy dissipation rate was chosen based on the assumption that, for adequate mixing to occur, the Kolmogorov length scale should be smaller than the average separation distance between clay particles so that all clay particles have similar exposure to coagulant precipitate. Mathematically, this can be stated as $\eta \leq \Lambda$. Substituting Equation 2.12 and Equation 2.16 (solved for Λ) into this inequality and solving for energy dis-

sipation rate results in an equation for the minimum energy dissipation rate for a given concentration of clay:

$$\varepsilon_{\mathrm{RM}} \geq \frac{\nu^3}{d_{\mathrm{P}}^4 \left(\frac{\pi}{6}\frac{\rho_{\mathrm{P}}}{C_{\mathrm{P}}}\right)^{4/3}}. \tag{2.28}$$

In calculating the design energy dissipation for rapid mix, the kinematic viscosity was assumed to be 1 mm^2/s and ρ_{P} was taken as 2.65 $\mathrm{g/cm}^3$, representative of the kaolinite particles used in this study. The value of C_{P} was taken to be 1,000 NTU, because the rapid mix intensity is set by the maximum particle concentration that would be treated by a water treatment plant. In order to convert the turbidity to a mass per volume concentration as required by Equation 2.28, a proportionality of 100 mg/L = 68 NTU was used (Wei et al., 2015). The diameter of the clay was set as 7 μm based on findings of Wei et al. (2015). The minimum energy dissipation rate was calculated to be 45 mW/kg, equivalent to a G value of 212 s^{-1} (assuming ν = 1 $\mathrm{mm/s}^2$). The minimum energy dissipation rate for effective rapid mix is extremely sensitive to the number of particles in the raw water. If the mean clay diameter were reduced to 4 μm, then the minimum energy dissipation rate would increase to over 400 mW/kg and that value was used to guide the rapid mix design.

The inner diameter of the orifice can be derived from the equation for the maximum energy dissipation encountered in a jet. The relationship for the maximum energy dissipation rate in a jet is based on the proportionality described in Equation 2.13, and thus can be approximated as Equation 2.29:

$$\varepsilon_{\mathrm{Max}} = \frac{\left(\Pi_{\mathrm{Jet\ Round}} V_{\mathrm{Jet}}\right)^3}{D_{\mathrm{Jet}}}, \tag{2.29}$$

where V_{Jet} is the average jet velocity, D_{Jet} is the diameter of the jet, and $\Pi_{\text{Jet Round}}$ is a coefficient related to the rate at which kinetic energy is transformed to thermal energy in a turbulent round jet and is equal to 0.5. The value of $\Pi_{\text{Jet Round}}$ was found from data gathered by Baldyga et al. (1995). In this article, the authors found the maximum energy dissipation rate (ε_{Max}) in a jet exiting an orifice at four different velocities. The value of $\Pi_{\text{Jet Round}}$ was thus found by solving Equation 2.29 for $\Pi_{\text{Jet Round}}$ and substituting the experimental values. The calculated values of $\Pi_{\text{Jet Round}}$ were between 0.47 and 0.49, so $\Pi_{\text{Jet Round}}$ was rounded to an approximation of 0.5.

Using the continuity of flow equation, $Q = VA$, where $A = \frac{\pi D^2}{4}$, Equation 2.29 can be rewritten as Equation 2.30:

$$\varepsilon_{\text{Max}} = \frac{\left(\Pi_{\text{Jet Round}} \frac{4Q}{\pi D_{\text{Jet}}^2}\right)^3}{D_{\text{Jet}}}. \tag{2.30}$$

The area of a round jet can be expressed as the product of the area of the orifice and the ratio of the *vena contracta* area to the orifice area (contraction coefficient), Π_{VC}, which is 0.62 (Finnemore and Franzini, 2002). Because the area of a circle is proportional to the diameter squared, the diameter of the jet can then be written as Equation 2.31:

$$D_{\text{Jet}} = D_{\text{Orifice}} \sqrt{\Pi_{\text{VC}}}. \tag{2.31}$$

Substituting Equation 2.31 in for D_{Jet} in Equation 2.30 and solving for D_{Orifice} yields Equation 2.32, an expression for the largest possible orifice diameter that can be used to achieve the target energy dissipation rate.

$$D_{\text{Orifice}} = \left(\frac{4Q\Pi_{\text{Jet Round}}}{\pi \varepsilon_{\text{Max}}^{1/3}} \right)^{3/7} \frac{1}{\sqrt{\Pi_{\text{VC}}}} \tag{2.32}$$

Based on the chosen flow rate of 109 mL/s and the minimum required maximum energy dissipation rate of 400 mW/kg, D_{Orifice} must be no larger than 2.39 cm (0.94 in) according to Equation 2.32. The orifice was thus chosen to be 1.88 cm (0.74 in). Using Equation 2.29, the maximum energy dissipation rate in the chosen rapid mix orifice size is about 514 mW/kg, and corresponds to a G value of 717 s^{-1}. This is within the typical range for mechanically-mixed rapid mix (600 – 1,000 s^{-1}), but lower than the typical range for in-line rapid mixing (3,000 – 5,000 s^{-1}) (Mihelcic and Zimmerman, 2010).

In order to verify that the hydraulic component of the apparatus design was valid, the head loss predicted through the flocculator was calculated and compared with the measured head loss through the system. The head loss through the flocculator was calculated as the sum of major and minor losses. Minor losses were computed according to the minor loss equation (Equation 2.20). In order to find the K value for the constrictions, an equation based on the conservation of momentum and the conservation of mass was used:

$$K_e = \left(\frac{A_{\text{Out}}}{A_{\text{In}}} - 1 \right)^2, \tag{2.33}$$

where A_{In} is the area of the constricted flow and A_{Out} is the area of the unconstricted flow (Granger, 1995). The value of A_{Out} is easily found, because it is the area of a circle with a diameter of 3.18 cm (1.25 in): 7.92 cm^2. Since A_{In} corresponds to the condition when the tube is compressed as in Figure 2.4, its calculation is not as simple.

For the experiments in this study, the tubing was constricted to an inner width, W, of 0.93 cm (0.36 in). Maintaining the assumption that the average circumference is unchanged by constriction and adding the assumption that the wall thickness is also conserved results in the assumption that the inner circumference of the tubing is conserved. Based on this assumption, A_{In} can be calculated.

To begin, the inner circumference is equal to $C_{\text{Inner}} = \pi D_{\text{I}} = 9.98$ cm. The length of the constriction, L, is then equal to the inner circumference minus the circumference of the two semicircles at the ends of the constricted tube, which have a diameter of W (0.93 cm), divided by two: $L = \frac{C_{\text{Inner}} - \pi W}{2} = 3.54\,\text{cm}$. As represented in Equation 2.25, the area is then $A_{\text{In}} = WL + \frac{\pi}{4}W^2 = 3.94\,\text{cm}^2$. Substituting the values for A_{In} and A_{Out} into Equation 2.33, the value of K for a single constriction is found to be 1.019. This value can vary, depending on the constriction width employed.

Taking the value of K for the entire flocculator to be the number of flow expansions (349) times the value of K for a single flow expansion (1.019) and the velocity in the tubing to be the flow rate in the tubing (109 mL/s) divided by the area of the tubing, $V = \frac{109\ \text{mL/s}}{7.92\ \text{cm}^2} = 13.8$ cm/s, the total minor loss was calculated to be 34.38 cm.

The major losses in the flocculator were calculated using the Darcy-Weisbach equation (Granger, 1995). This is shown in Equation 2.34:

$$h_f = f\frac{L}{D}\frac{V^2}{2g} = f\frac{8}{g\pi^2}\frac{Q^2}{D^4}. \tag{2.34}$$

In order to find the friction factor, f, in Equation 2.34, the Swamee Jain equation

for friction factor in a full-flowing circular pipe was used:

$$f = 0.25\left[\log_{10}\left(\frac{\varepsilon_{\text{Pipe}}}{3.7D} + \frac{5.74}{\text{Re}^{0.9}}\right)\right]^{-2}, \tag{2.35}$$

where $\varepsilon_{\text{Pipe}}$ is the roughness of the pipe, D is the pipe diameter, and Re is the Reynolds number of flow in the pipe (Swamee and Jain, 1976). The tubing was assumed to be smooth, so the value of $\varepsilon_{\text{Pipe}}$ was taken as 0. Using this value as well as the pipe diameter of 3.18 cm (1.25 in) and the Reynolds number of 4,371, the value of f was found to be 0.04. With the design diameter of 3.18 cm (1.25 in) and the design flow rate of 109 mL/s, the major losses were then calculated to be 6.80 cm.

Last, the minor losses associated with the rapid mix orifice were calculated by using Equation 2.20 and Equation 2.33, as had been done for the minor losses in the flocculator. In solving Equation 2.33 for K of the rapid mix orifice, the value of A_{Out} was the same as for the flocculator, 7.92 cm^2. The value of A_{In} was taken as the area of the vena contracta after the orifice, $A_{\text{In}} = \Pi_{\text{VC}}\frac{\pi}{4}D_{\text{RM}}^2$. With $\Pi_{\text{VC}} = 0.62$ and $D_{\text{Orifice}} = 1.88$ cm, the value of A_{In} was found to be 1.71 cm^2. Substituting A_{In} and A_{Out} into Equation 2.33, the value of K was 13. Using this value of K and the velocity in the flocculator, 13.8 cm/s, the head loss due to the rapid mix was 1.27 cm according to Equation 2.20.

Based on the above calculations, the total head loss through the flocculator was expected to be around 42.5 cm. Measurements showed the actual head loss to be about 32 cm. The value of K was highly sensitive to measurement of the constriction width, and thus the discrepancy can likely be attributed to inaccuracies in setting and measuring the constriction width. Additionally, some bow-

ing outward by the vertical supports likely meant that there were lower values of K in some of the constrictions in the middle of the flocculator. If the average constriction width had been underestimated by 1 mm (0.04 in), the calculated head loss would be 32 cm.

2.4 Experimental Protocols

A diagram depicting the layout of the experimental apparatus and the path of the flow is given in Figure 2.5. As shown, the water was treated prior to being used in the experiments. For pretreatment, the water was first passed through a granular activated carbon (GAC) filter in order to reduce the concentration of natural organic matter (NOM) present in Cornell University tap water. The prior study on laminar flocculation had some variation in performance trends that was hypothesized to be due to NOM variability in the tap water and concomitant consumption of coagulant (Swetland et al., 2014). On average, Cornell University tap water has a pH of 7.36, a turbidity of 0.062 NTU, a total hardness of 150 mg/L, a total alkalinity of 131 mg/L, and a dissolved organic carbon (DOC) concentration of 1.83 mg/L (BP-MWS et al., 2014). After treatment with activated carbon, the water was then aerated to strip out supersaturated dissolved oxygen, which can form bubbles when depressurized, causing disruptions to sedimentation.

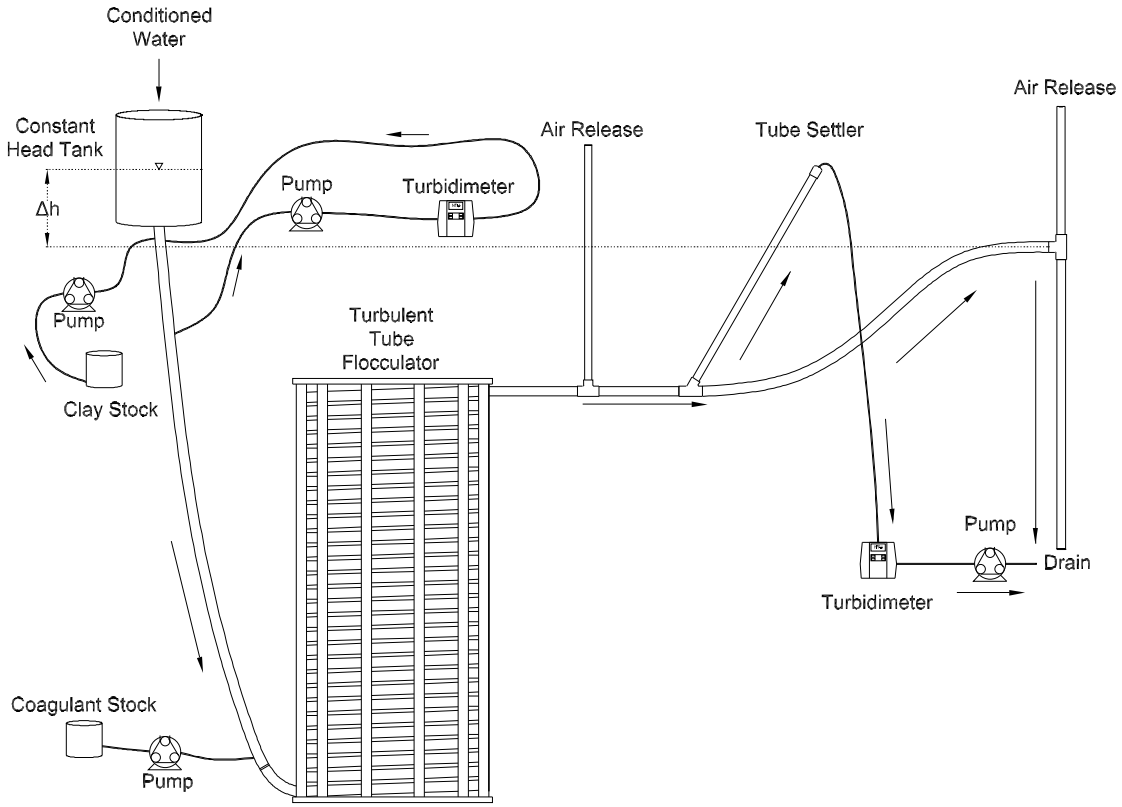

Figure 2.5: Diagram of Flow Path

The conditioned water was then sent to a constant head tank, where its level was controlled by a float valve. The flow rate through the system was controlled by adjusting the elevation difference between the water level in the constant head tank and the level of water at the effluent drain. The drain had an opening to the atmosphere so that a free surface (i.e., area with no pressure head) was formed and the outlet water level would be constant.

A portion of the water flowing down out of the constant head tank was sampled with a peristaltic pump into a turbidimeter, where it was analyzed for turbidity and then reintroduced upstream of the sampling point. At approximately the same point at which the sampled water was returned to the flow, a

concentrated suspension of kaolinite clay (R.T. Vanderbilt Co., Inc., Norwalk, Connecticut) was injected by means of a peristaltic pump. The flow rate of this pump was controlled by a PID control system that took the influent turbidity measurement as an input. For the initial experiments, the influent turbidity was set to be 150 nephelometric turbidity units (NTU).

Just before the turbid flow reached the flocculator, it was dosed with coagulant by a peristaltic pump. The coagulant used in this research was poly-aluminum chloride (PACl) manufactured by the Holland Company, Inc., Adams, Massachusetts. The coagulant was injected into the center of the tubing just before the rapid mix, which was the orifice within the tubing described above. The exact dose of coagulant was measured by placing the PACl stock on a balance equipped with a serial port. The mass was recorded at 5 s intervals during experiments and, with the knowledge of the density of the coagulant stock, was used to get an accurate measurement of the coagulant dose.

After the suspension had been flocculated (residence time of about 7 minutes), a continuous sample of the flocculated suspension was passed through a tube settler and the settled effluent turbidity was used as a measure of flocculation performance. Prior to settling, the flow passed an air release, a vertical tube with a free surface that allowed bubbles floating along the top of the tubing to rise out of the flow. Air bubbles were removed to avoid interference with the sedimentation process and the nepehlometric turbidity readings.

Sedimentation was accomplished by an inclined tube settler. A fraction of the flocculator flow was drawn through the tube settler by a peristaltic pump. The remainder of the flow went to a drain, carrying with it the particles that settled in the tube settler. The flow rate through the tube settler was set by the

desired capture velocity for the experiment. The equation for this flow rate is given by Equation 2.36:

$$Q_{\text{Settle}} = \frac{\pi}{4} D^2 V_c \left(\frac{L}{D} \cos \alpha + \sin \alpha \right) \tag{2.36}$$

where V_c is the capture velocity, L is the length of the tube settler, D is the diameter of the tube settler, and α is the angle of inclination of the tube settler (Schulz and Okun, 1984). The experimental tube settler had a length of 86 cm, a diameter of 2.66 cm, an angle of inclination of 60° (giving a settling depth of 5.32 cm), and a capture velocity of 0.12 mm/s, resulting in a flow rate of 1.14 mL/s according to Equation 2.36. The effluent from the tube settler was analyzed in an inline turbidimeter and then sent to the drain. In these experiments, control of pumps and data acquisition were accomplished using the ProCoDA (Process Control and Data Acquisition) software developed by Dr. Monroe Weber-Shirk for the AguaClara Program at Cornell University (Weber-Shirk, 2015).

2.5 Results

At the end of each experiment, data like those shown in Figure 2.6 were analyzed. The red line in Figure 2.6 shows the turbidity of the water entering the apparatus which was held approximately constant at 150 NTU by PID control. The green line in Figure 2.6 shows the turbidity of settled water (settled at capture velocity of 0.12 mm/s) from the apparatus. With the dose of PACl at 0.53 mg/L as aluminum, the performance was good, reducing the turbidity by almost 1.5 orders of magnitude. The initial spike in effluent turbidity was from the prior experiment.

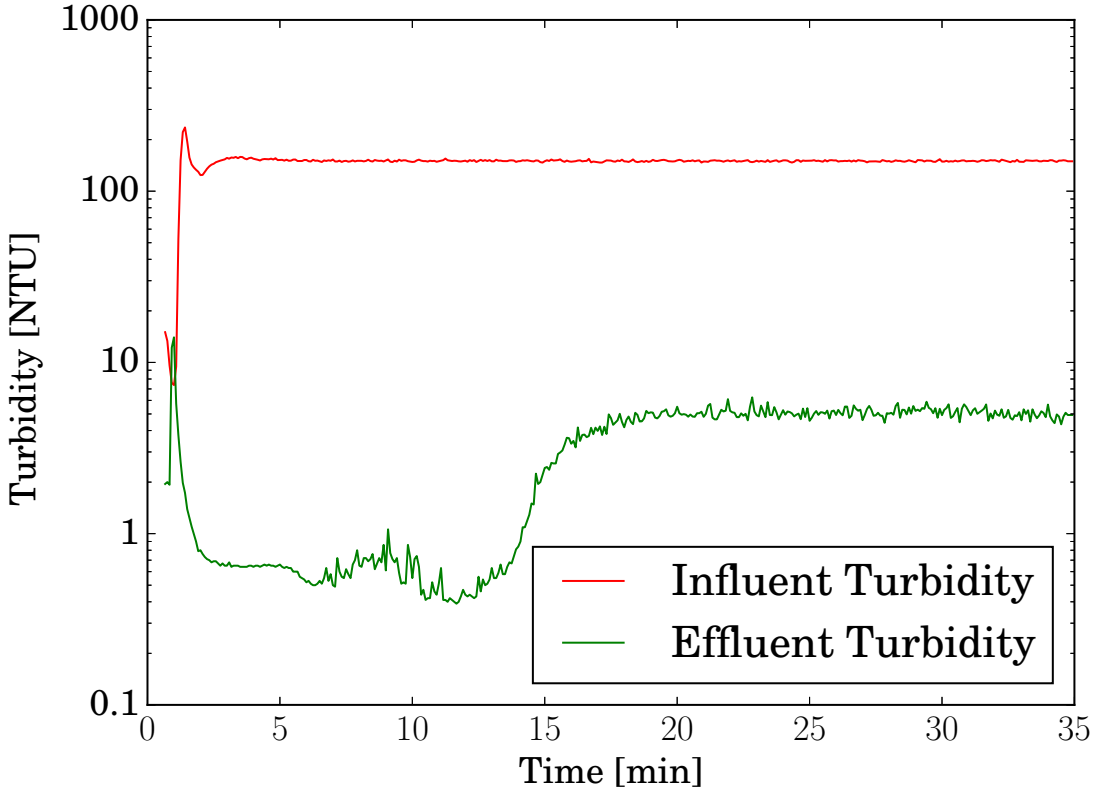

Figure 2.6: Example of Data from Single Experiment (PACl Dose 0.53 mg/L as Aluminum)

After a number of experiments at different coagulant doses were run, the data were analyzed to observe overall trends in performance. Performance was made dimensionless by dividing the settled effluent turbidity by the influent turbidity. The negative log (base 10) was then taken of this ratio to get pC^*:

$$\mathrm{p}C^* = -\log_{10}\left[\frac{\mathrm{EffluentTurbidity}}{\mathrm{InfluentTurbidity}}\right]. \tag{2.37}$$

In order to determine if the composite parameter was applicable to these experimental conditions, the Stokes number needed to be determined in order to ascertain if it was sufficiently low. The Stokes number is defined as

$$\mathrm{St} = \frac{\tau_r}{\tau_\eta}, \tag{2.38}$$

where τ_r is the response time, or the time it takes the particle to accelerate to a new surrounding velocity, and τ_η is the characteristic time of the flow, which in this case is the Kolmogorov time scale, the characteristic time of the smallest motions of turbulent flow (Crowe, 2005).

The response time, τ_r, is defined as

$$\tau_r = \left(\frac{\rho_\mathrm{P}}{\rho} - 1\right)\frac{d_\mathrm{P}^2}{18\nu}, / \tag{2.39}$$

where ρ and ν are the density and kinematic viscosity of the fluid (Crowe, 2005). Likewise, the Kolmogorov time scale is defined as

$$\tau_\eta = \sqrt{\frac{\nu}{\varepsilon}} = \frac{1}{G} \tag{2.40}$$

(Tennekes and Lumley, 1972). Solving for the Stokes number assuming a kaolinite particle diameter of 7 μm, a kaolinite particle density of 2.65 g/cm^3, a density of water of 1 g/cm^3, a kinematic viscosity of water of 1 mm/s^2, and an energy dissipation rate of 15 mW/kg, the value was found to be 5.5×10^{-4}, which is far less than 1, indicating that kaolinite primary particles will accelerate with the fluid. Thus, the composite parameter is applicable to kaolinite particles in water at these mixing conditions.

The coagulant dose for each experiment was converted to the approximate composite parameter given in Equation 2.18. In order to do this, values for

ϕ_0 and Γ needed to be calculated. Both values were calculated in the manner described by Swetland et al. (2014).

The initial value of the volume fraction of particles, ϕ_0, was determined by considering the contribution of both kaolinite clay and PACl precipitates to the initial particle volume fraction in the flocculator:

$$\phi_0 = \frac{C_{\text{Coag}} R_{\text{Clay}}}{\rho_{\text{Coag}}} + \frac{C_{\text{Clay}_0}}{\rho_{\text{Clay}}}, \tag{2.41}$$

where C_{Coag} is the concentration of coagulant, C_{Clay_0} is the concentration of the clay in the influent (as $\frac{\text{Mass}}{\text{Volume}}$), ρ_{Coag} is the density of the coagulant precipitates, ρ_{Clay} is the density of clay particles, and R_{Clay} is the fraction of coagulant precipitates that adhere to clay particles rather than the wall of the flocculator. The value of R_{Clay} is assumed to be the fraction of the total available surface area in the system that is associated with clay particles, or $\frac{\text{SA}_{\text{Clay}}}{\text{SA}_{\text{Clay}}+\text{SA}_{\text{Wall}}}$, which assumes that coagulant has equal affinity for clay particles and flocculator walls.

The value of fractional surface coverage of clay particles by coagulant precipitates, Γ, was modeled by Swetland et al. (2014) using a Poisson distribution to account for the possibility of coagulant precipitates adhering on top of previously adhered coagulant precipitates rather than to the particle surface. Thus, Γ is calculated as

$$\Gamma = 1 - e^{-\frac{d_{\text{Coag}}^2}{\text{SA}_{\text{Clay}}} N_{\text{per Clay}} R_{\text{Clay}}}, \tag{2.42}$$

where d_{Coag} is the average diameter of coagulant precipitate primary particles, SA_{Clay} is the total surface area of clay particles in the suspension, $N_{\text{per Clay}}$ is the

average number of coagulant precipitates per clay particle, and R_{Clay} is the fraction of coagulant precipitates that adhere to clay particles as previously defined (Swetland et al., 2014). Using a Malvern Zetasizer Nano-ZS to analyze a 138.5 mg/L solution of PACl (as Aluminum), d_{Coag} was measured to be 20 nm (Garland, 2015). The value of $N_{\text{per Clay}}$ was estimated as the total volume of clay divided by the total volume of the coagulant,

$$N_{\text{per Clay}} = \frac{[C_{\text{Coag}} - C_{\text{Coag(aq)}}]\, \forall_{\text{Clay}}\, \rho_{\text{Clay}}}{\frac{\pi}{6} d_{\text{Coag}}^3 \rho_{\text{Coag}} C_{\text{Clay}_0}} \tag{2.43}$$

(Swetland et al., 2014).

Using the procedure described above, values of Γ (see Figure 2.7) and ϕ_0 (ranging from 9.6×10^{-5} to 1.1×10^{-4}) were found for each experiment. These values were then inserted, along with an average energy dissipation rate ($\overline{\varepsilon}$) of 7.4 mW/kg and a hydraulic residence time (θ) of 6.82 min, into Equation 2.18 to find the composite parameter for each experiment. Having done this, a plot of the overall change in performance with respect to coagulant dose was created, with performance in terms of pC^* as the ordinate and the coagulant dose and other relevant flocculation parameters included as the turbulent composite parameter for the abscissa (see Figure 2.8).

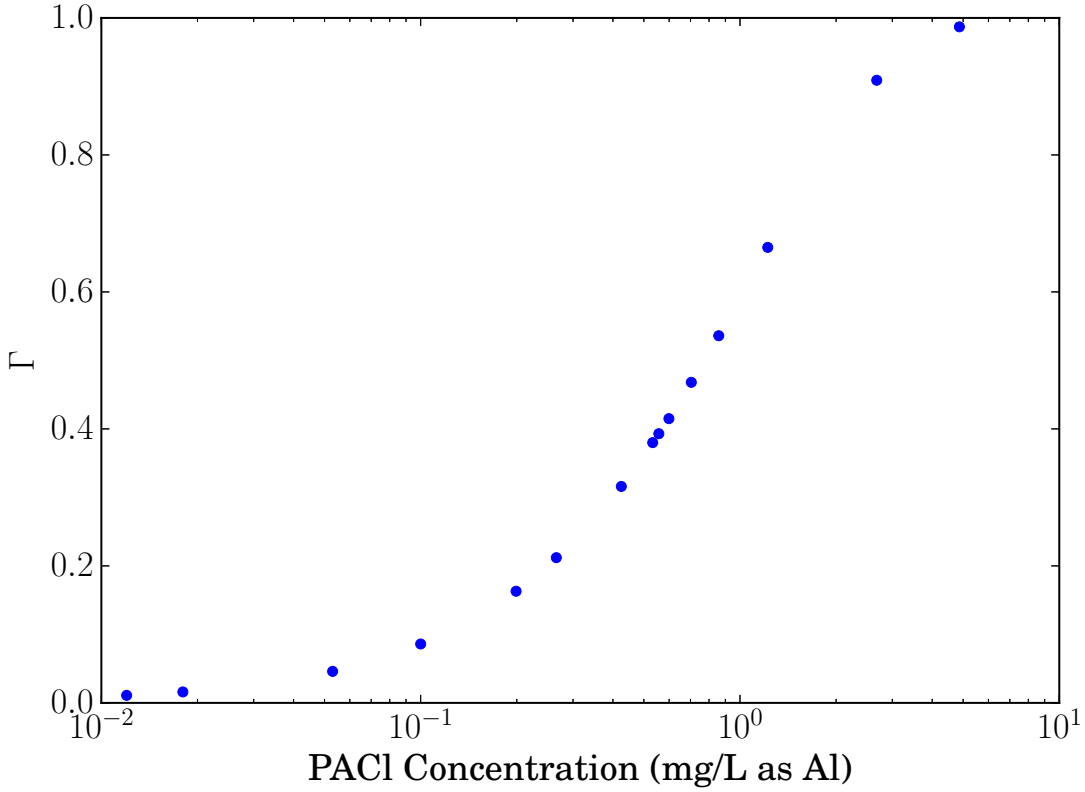

Figure 2.7: Value of Fractional Coverage of Clay Particles by PACl Precipitates Versus Concentration of PACl

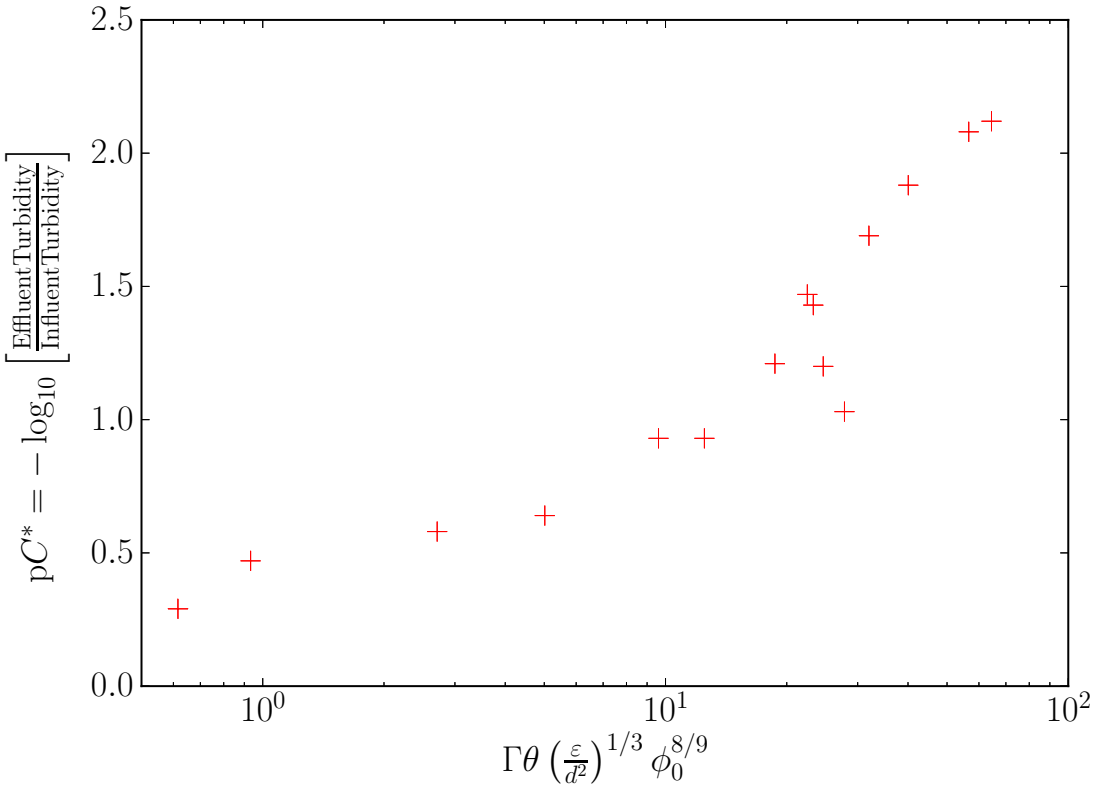

Figure 2.8: Data for Experiments at 150 NTU Influent Turbidity, 0.12 mm/s Capture Velocity, and varying Coagulant Doses

2.6 Discussion

Referring to Figure 2.8, a definite trend in the data can be seen. Namely, for sufficiently low coagulant doses (those where $\Gamma\theta\left(\frac{\bar{\varepsilon}}{d_P^2}\right)^{1/3}\phi_0^{8/9} < 10$), there is little change in performance with respect to coagulant dose. The lowest performance was achieved by the lowest coagulant dose (0.012 mg/L as aluminum), with a pC^* of 0.29. This approached the performance of flocculation with no coagulant added, which had a pC^* of 0.25.

In the middle range of coagulant doses, where the composite parameter was roughly between 10 and 50 (coagulant doses between 0.27 mg/L and 1.22 mg/L as aluminum), there was an approximately linear relationship between performance and coagulant dose (on the log-log plot).

The highest dose of 4.87 mg/L as aluminum resulted in only slightly better performance than the next highest dose of 2.68 mg/L as aluminum. This small improvement in performance with increasing coagulant dose may be due to adequate coverage of the clay particles by coagulant such that additional coagulant dose has a negligible effect on attachment efficiency.

2.7 Summaries

In this study, a theoretical basis for the development of a predictive model for flocculation in turbulent flows was described. This analysis led to the proposal of a new dimensionless composite parameter, $\Gamma\theta\left(\frac{\bar{\varepsilon}}{d_P^2}\right)^{1/3}\phi_0^{8/9}$, to describe flocculation in turbulent conditions. In order to test the usefulness of this parameter, the design of a lab scale turbulent tube flocculator was outlined. This flocculator, which was intended to represent flow conditions in a baffled hydraulic flocculator, was tested at a number of coagulant doses with an influent turbidity of 150 NTU followed by a tube settler with a capture velocity of 0.12 mm/s. Results from these experiments showed settled water turbidity variations consistent with expectations for very low to full surface coverage of colloids with coagulant. The utility of the composite parameter awaits confirmation by future experiments in which initial turbidity, capture velocity, fluid residence time, and energy dissipation rate will be changed in addition to coagulant dose. The

experimental apparatus described above permits each of these variables to be modified over a wide range. If the composite parameter captures the mechanistic effects of the characteristics that control coagulation in turbulent flow, data from such experiments should converge with the curve defined by the initial results presented in this paper.

Chapter 3

Conclusions and Recommendations

In this thesis, a dimensionless composite parameter of the form $\Gamma\theta\left(\frac{\bar{\varepsilon}}{d^2}\right)^{1/3}\phi_0^{8/9}$ is proposed to explain turbulent flocculator performance. In order to test the usefulness of this parameter, a turbulent, lab-scale hydraulic flocculator was designed, as outlined in this paper. The apparatus constructed according to this design achieved the design constraints of being able to achieve turbulent flow (Re $> 4,000$), having a high Péclet number (90.9), and having a variable energy dissipation rate that can achieve mixing intensities higher than typically used in hydraulic flocculator designs ($G > 100\ \mathrm{s}^{-1}$ or $\overline{\varepsilon} > 10\ \frac{\mathrm{mW}}{\mathrm{kg}}$).

Preliminary tests were conducted with this flocculator with an influent turbididty of 150 NTU ($\phi_0 \approx 1 \times 10^{-4}$), a hydraulic residence time (θ) of 6.82 min, an average energy dissipation rate ($\overline{\varepsilon}$) of 7.4 mW/kg, a capture velocity of 0.12 mm/s, and a range of coagulant doses ($0 < \Gamma < 1$), leading to a range of values of the composite parameter from 0.6 to 64.5. Results from these preliminary experiments showed several regimes of performance. For values of the composite

parameter below about 10, performance improved only gradually with increasing values of the composite parameter. For values between around 10 and 50, performance increased at a much greater rate with increases in the parameter, and the relationship was linear on a log-log plot. For values of the composite parameter greater than 50, increases in the composite parameter were attended by only modest gains in flocculation performance. These data are not conclusive, and further experiments are needed to validate the utility of the proposed composite parameter.

Future work, then, is needed to test flocculator performance over a broad range of values of the composite parameter, with individual components of the composite parameter being varied. Varying coagulant dose will vary Γ, varying constriction width or flow rate will change $\bar{\varepsilon}$, varying influent turbidity and coagulant dose will change ϕ_0, and varying the flow rate or the length of the flocculator will change θ. Varying the tube settler capture velocity will characterize the size range of small flocs produced under each set of conditions. A battery of experiments in which all of these variables have a wide range of values will provide a dataset that should hopefully collapse to one line when plotted against the composite parameter, if it is correct. If this is not the case, further refinement will be made to the composite parameter.

Building upon the composite parameter, an integrated predictive model of turbulent flocculator performance must be derived. The goal for this model is to accurately represent the dominant mechanisms of flocculation using as inputs the characteristics of the flocculator and sedimentation tank as well as the influent water to predict the turbidity leaving the sedimentation tank. This model will be tailored to the data gathered to verify the composite parameter, using

composite parameter as a variable as well as sedimentation tank capture velocity. Having successfully developed this model, additional phenomena will be considered for inclusion in the model, such as the effect of floc break-up and consumption of coagulant by natural organic matter. Once the model reaches a state where it is able to describe flocculation in real conditions, it will be tested on real, municipal-scale flocculators in Honduras.

Bibliography

Baldyga, J., Bourne, J. R., and Gholap, R. V. (1995). The influence of viscosity on mixing in jet reactors. *Chemical Engineering Science*, 50(12):1877–1880.

BP-MWS, CIWS, and CUWS (2014). Drinking Water Quality Report 2014. Technical report, Bolton Point Municipal Water System, City of Ithaca Water System, Cornell University Water System, Ithaca, NY.

Cleasby, J. (1984). Is Velocity Gradient a Valid Turbulent Flocculation Parameter? *Journal of Environmental Engineering*, 110(5):875–897.

Crowe, C., editor (2005). *Multiphase Flow Handbook*. Mechanical Engineering Series. CRC Press.

Finnemore, E. J. and Franzini, J. B. (2002). *Fluid mechanics with engineering applications*. McGraw-Hill, Boston, 10th edition.

Garland, C. (2015). Size Measurement of PACl Precipitate Particles.

GLUMRB (2012). *Recommended Standards for Water Works*. 10 States Standards. Health Research, Inc., Health Education Services Dvision, Albany, NY, 2012 edition.

Granger, R. A. (1995). *Fluid Mechanics*. Dover Publications, New York.

Haarhoff, J. (1998). Design of Around-the-End Hydraulic Flocculators. *Journal of Water Supply: Research and Technology - Aqua*, 47(3):142–152.

Haarhoff, J. and van der Walt, J. J. (2001). Towards Optimal Design Parameters for Around-the-End Hydraulic Flocculators. *Journal of Water Supply: Research and Technology - Aqua*, 50(3):149–159.

Kim, D.-G. (2007). Numerical analysis of free flow past a sluice gate. *KSCE Journal of Civil Engineering*, 11(2):127–132.

Kotsovinos, N. E. (1976). A note on the spreading rate and virtual origin of a plane turbulent jet. *Journal of Fluid Mechanics*, 77(02):305–311.

Mihelcic, J. R. and Zimmerman, J. B., editors (2010). *Environmental engineering: fundamentals, sustainability, design*. Wiley, Hoboken, NJ.

Schulz, C. R. and Okun, D. A. (1984). *Surface water treatment for communities in developing countries*. Wiley, New York.

Swamee, P. K. and Jain, A. K. (1976). Explicit Equations for Pipe-Flow Problems. *Journal of the Hydraulics Division, Proceedings of the American Society of Civil Engineers*, 102(5):657–664.

Swetland, K. A., Weber-Shirk, M. L., and Lion, L. W. (2014). Flocculation-Sedimentation Performance Model for Laminar-Flow Hydraulic Flocculation with Polyaluminum Chloride and Aluminum Sulfate Coagulants. *Journal of Environmental Engineering*, 140(3):04014002.

Tennekes, H. and Lumley, J. (1972). *A First Course in Turbulence*. MIT Press, Cambridge, Mass.

Weber-Shirk, M. L. (2015). ProCoDA: An Automated Method for Testing Process Parameters.

Weber-Shirk, M. L. and Lion, L. W. (2010). Flocculation model and collision potential for reactors with flows characterized by high Peclet numbers. *Water Research*, 44(18):5180–5187.

Wei, N., Zhang, Z., Liu, D., Wu, Y., Wang, J., and Wang, Q. (2015). Coagulation behavior of polyaluminum chloride: Effects of pH and coagulant dosage. *Chinese Journal of Chemical Engineering*, 23(6):1041–1046.